THE ASTROPHYSICAL JOURNAL, 454:429–441, 1995 November 20

IMPROVED CALCULATIONS OF THE EQUILIBRIUM ABUNDANCES OF HEAVY ELEMENTS SUPPORTED BY RADIATIVE LEVITATION IN THE ATMOSPHERES OF HOT DA WHITE DWARFS

P. CHAYER,[1] S. VENNES,[1] A. K. PRADHAN,[2] P. THEJLL,[3] A. BEAUCHAMP,[4] G. FONTAINE,[4] AND F. WESEMAEL[4]

Received 1995 March 20; accepted 1995 June 2

ABSTRACT

We present revised estimates of the equilibrium abundances of heavy elements supported by radiative levitation in the atmospheres of hot DA white dwarfs. We emphasize, in particular, the role of trace pollutants that may be present in the background plasma, an effect which has been heretofore neglected. We take advantage of the availability of a table of detailed monochromatic opacities calculated for a plasma made of H and containing small amounts of C, N, O, and Fe to illustrate how the equilibrium abundances of levitating elements react to the flux redistribution caused by the addition of these small traces of opaque material. We address this problem through a model-atmosphere approach, which gives an exact description of the flux redistribution. We also consider two other improvements: a more sophisticated treatment of the momentum redistribution process an ion experiences following a photoexcitation and use of an upgraded value for the line profile width associated with pressure broadening. These improvements bring the present results to the state-of-the-art level in the context of *equilibrium* radiative levitation theory.

Subject headings: atomic processes — diffusion — stars: abundances — white dwarfs

1. INTRODUCTION

The presence of pollutants in the high-gravity atmospheres of white dwarfs has received considerable attention in the last several years, thanks to important discoveries made in the UV, far-UV, and extreme-UV spectral ranges. On the basis of such observations, quantitative abundance analyses have revealed, so far, the presence of C, N, O, Si, Fe, and Ni in a handful of bright hot dwarfs.[5] To understand better how radiative levitation could potentially account for these and other possible atmospheric contaminants, Chayer, Fontaine, & Wesemael (1995; hereafter CFW) recently presented the results of detailed calculations of radiative accelerations and equilibrium abundances for several elements in the envelopes of hot DA and DO/DB white dwarf models. Using the extensive and homogeneous atomic data provided by TOPBASE (Cunto & Mendoza 1992), associated with the Opacity Project (Seaton et al. 1992), CFW present results for C, N, O, Ne, Na, Mg, Al, Si, S, Ar, Ca, and Fe, i.e., for all heavy elements contained in the database. Chayer et al. (1994) carry out similar calculations for Fe and Ni in hot DA stars using the data compiled by Kurucz (1991, 1992) for the Fe-group elements. These two sets of computations use equilibrium surface abundances derived under the assumption of a strict balance between the radiative acceleration on a given element and the effective gravity at the Rosseland photosphere. This *equilibrium approach* which ignores the potential influence of other, competing mechanisms (e.g., stellar winds or accretion), constitutes but the first step toward understanding the observed patterns of trace heavy elements in hot white dwarfs.

CFW (see also Chayer et al. 1994) have pointed out that the most significant aspect of this equilibrium theory which remains to be addressed in the white dwarf context, is the problem of flux blocking (or, more properly, flux redistribution) resulting from the simultaneous presence of traces of several different heavy elements in the atmospheres of hot stars. Indeed, they adopt a simplified approach in their calculations (as, to our knowledge, in all others previously carried out). They consider only one levitating element at a given time and disregard the effects of other contaminants. In this approach, the radiation flux available to a particular element is specified only by the minimal opacity of the dominant atmospheric constituent (e.g., pure H in DA stars) and not, as it should be in the presence of a mixture, by the opacity from the simultaneous presence of the dominant constituent and all other levitating elements. This flux specification is potentially a serious problem because the extra opacity from the other trace contaminants (particularly that from Fe-group elements) may reduce or increase (through redistribution) the flux available across the line spectrum of an element and, consequently, alter the transfer of momentum from the radiation field to the element. This effect may significantly affect the *relative* abundances of the various elements supported by radiative levitation in a given star. This is a result of potential importance for the interpretation of the observations.

In order to assess the importance of this effect, we have carried out exploratory calculations in DA models based on a representative mixture of C, N, O, and Fe that, together with the dominant element (H here), may provide a more realistic background monochromatic opacity than that provided by H alone. We point out, at the outset, that the present calculations can only be considered as indicative and representative of the real situation. Indeed, a full, self-consistent computation is not yet possible because we do not know a priori the exact chemi-

[1] Center for EUV Astrophysics, 2150 Kittredge Street, University of California, Berkeley, Berkeley, CA 94720-5030; chayer, vennes@cea.berkeley.edu.
[2] Department of Astronomy, Ohio State University, Columbus, OH 43210–1106; pradhan@payne.mps.ohio-state.edu.
[3] Niels Bohr Institute, Blegdamsvej 17, DK-2100, København Ø, Denmark; thejll@nordita.dk.
[4] Département de Physique, Université de Montréal, C.P. 6128, Succ. Centre-Ville, Montréal, Québec, Canada, H3C 3J7; beaucham, fontaine, wesemael@astro.umontreal.ca.
[5] Wesemael, Henry, & Shipman (1984); Sion, Liebert, & Wesemael (1985); Vennes, Thejll, & Shipman (1991); Vennes et al. (1992); Holberg et al. (1993, 1994); Vidal-Madjar et al. (1994); Napiwotzki et al. (1993); Werner, Heber, & Fleming (1994); Werner & Dreizler (1994); Werner, Dreizler, & Wolff (1995); Chayer, Fontaine, & Wesemael (1995).

cal composition of the mixture of heavy elements that may pollute the atmosphere of a given hot white dwarf. For instance, it is highly likely that elements other than C, N, O, Si, Fe, and Ni, yet to be formally identified, are nevertheless present in the atmospheres of some hot DA stars (see, e.g., Vennes et al. 1989; Vennes 1992). Also, from the analysis of CFW, the composition of this mixture of contaminants clearly varies from one star to another, a fact they interpret as a signature of other, competing mechanisms.

With this caveat in mind, and in an exploratory spirit, we compute here the expected equilibrium abundances of the 12 heavy elements available in TOPBASE at the Rosseland photosphere of atmospheric models of DA stars. This is a departure from the work of CFW, where only envelope models were considered, and is required because of the importance of an exact description of the flux redistribution in the presence of the additional opacity of metals, which will be considered later in this paper. To gain some insight into this process, and to allow us to assess the validity of the CFW envelope calculations, we first compute a grid of pure-H model atmospheres and synthetic spectra to calculate representative equilibrium abundances of levitating elements in hot, pure-H atmospheres. In a second step, we consider the effects of including trace contaminants in the assumed chemical composition of the atmospheric layers and make use of a small grid of detailed, blanketed model atmospheres for our mixture of H, C, N, O, and Fe. In this calculation, we use the opacity of a *fixed* mixture of H, C, N, O, and Fe whose detailed monochromatic structure has been computed in advance on a small grid in the electron density–temperature plane. This grid allows us to explore a sufficiently large subset of the stellar models considered by CFW, making detailed comparisons with the former results possible.

Finally, in § 3, we further upgrade our approach to equilibrium radiative levitation theory in white dwarfs by combining the above model-atmosphere description with an implementation of the momentum redistribution process recently discussed by Gonzalez et al. (1995). This process is related to the probability that an ion that has just absorbed a photon spends its newly gained momentum either in its initial ionization state i or in the higher ionization state $i + 1$. As mentioned by CFW (their § 4), this consideration, along with the other questions considered above, is the last remaining major improvement that needs to be tackled in the framework of equilibrium radiative levitation theory. As such, the present paper can be considered as a complement to, and an extension of, the work of CFW, particularly with respect to the observable surface abundances. We summarize our results in the last section.

2. MODEL-ATMOSPHERE APPROACH

2.1. *Pure-Hydrogen Models*

The computation of the total radiative acceleration on a given trace element is based on equation (1) of CFW, except that the background monochromatic Eddington flux, $H_\nu(b)$, is evaluated through the full solution of the radiative transfer problem in the atmospheric layers instead of relying on approximations only formally valid at large optical depths. This approach is similar to the one followed by Bergeron et al. (1988) in the context of hot B subdwarfs. We compute the equilibrium abundances of levitating elements at the Rosseland photosphere ($\tau_R = \frac{2}{3}$) of our model atmospheres, as these abundances are *representative* of the observable values (see Chayer et al. 1998a; Chayer, Fontaine, & Wesemael 1989b; and CFW for a discussion of this point). In order to provide a comparison point with the results of CFW as well as with the results of more complicated models below, we first consider the case of *pure*-H atmosphere models.

Our grid consists of standard, pure-H, line-blanketed, LTE models computed for four values of the surface gravity, $\log g = 7.0$, 7.5, 8.0, and 8.5, and 17 values of the effective temperature, in the range $20{,}000\ \mathrm{K} \leq T_{\rm eff} \leq 100{,}000\ \mathrm{K}$, in steps of 5000 K. These model atmospheres are calculated using a modified version of the linearized code of Wesemael et al. (1980), which incorporates the occupation probability formalism of Hummer & Mihalas (1988) and other improvements. Some sample results are presented in Figure 1, which shows the distribution of the Eddington flux at the Rosseland photosphere ($\tau_R = \frac{2}{3}$) of pure-H model atmospheres (*dotted curves*) and pure-H model envelopes (*solid curves*) with $\log g = 7.5$ and $T_{\rm eff} = 40{,}000$, 70,000, and 100,000 K. The solid curves correspond to the approach of CFW and represent the background Eddington flux, namely,

$$H_\nu(b) = \frac{\kappa_R}{k_b(\nu)} \frac{dB_\nu}{dT} \frac{1}{16} \frac{R^2}{r^2} \frac{T_{\rm eff}^4}{T^3}, \tag{1}$$

where κ_R is the Rosseland mean opacity, B_ν is the Planck distribution, T is the temperature, R is the total radius of the star, r is the radial coordinate, and $T_{\rm eff}$ is the effective temperature. Not surprisingly, the flux distributions are different. Note, in particular, that these differences become very significant at X-ray frequencies, where the true flux is much larger than the approximate flux. However, given the definition of the Rosseland opacity, it should be pointed out that the basic relation,

$$\int_0^\infty H_\nu(b)\, d\nu = \frac{\sigma T_{\rm eff}^4}{4\pi}, \tag{2}$$

which is satisfied at large optical depths when our approximate expression for $H_\nu(b)$ is used, remains well verified even at $\tau_R = \frac{2}{3}$ (*solid curves*). We have, in fact, explicitly verified that this relation is satisfied to within 0.5% and better for *all* the surface fluxes used by CFW. Of course, even if the integral of the approximate flux satisfies equation (2) fairly well, this fact does not mean that the flux distribution itself is correct, as a cursory inspection of Figure 1 quickly reveals. However, it does mean that the two kinds of curves must cross, as shown in the figure. Thus, to a certain extent, as far as the total radiative acceleration on an element is concerned, a compensation effect exists between the frequency ranges where the approximate flux is smaller and the ranges where it is larger than the true flux. This effect, in part, led CFW to conjecture that their approach would lead to reasonable estimates of the surface abundances of radiatively levitating elements.

To a large extent, their expectation is borne out by the results of the detailed calculations of atmospheric equilibrium abundances based on the model-atmosphere approach used here. The result is shown in Figure 2, where the expected equilibrium surface abundances of levitating elements are shown as functions of the effective temperature and the surface gravity for pure-H DA models. The solid curves show the results of CFW, while the dashed curves correspond to the improved results obtained in the present study. The horizontal dotted line in each panel gives the cosmic-number abundance of the

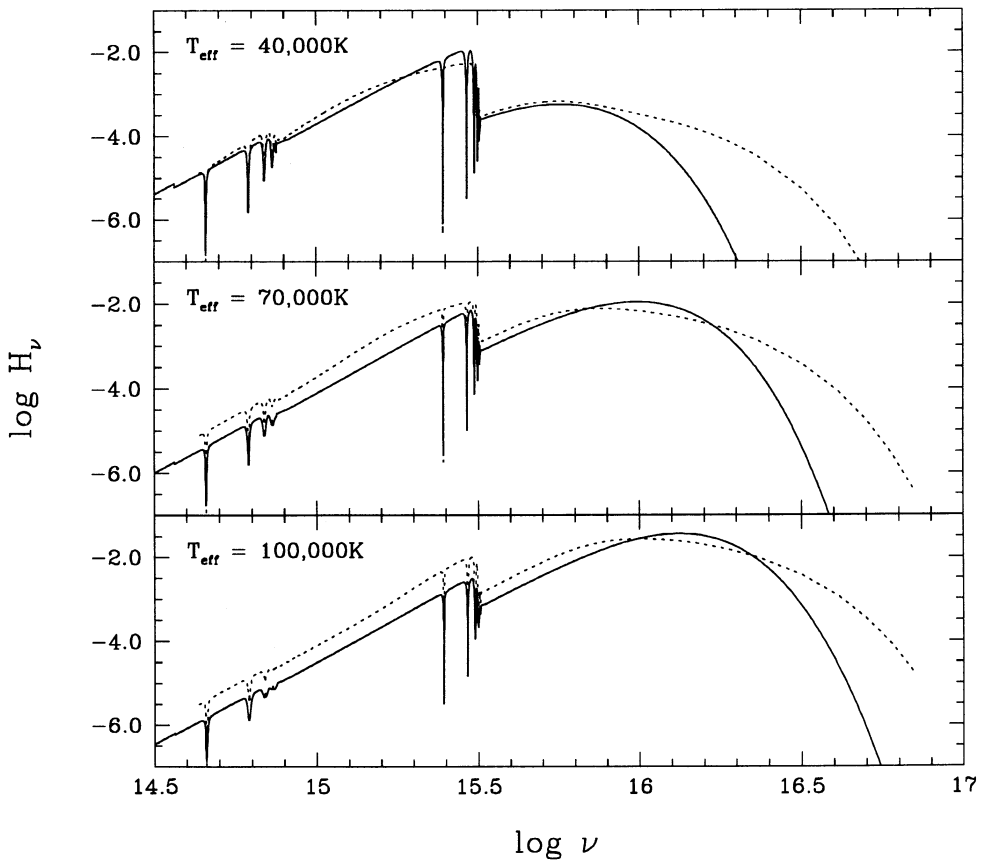

FIG. 1.—Eddington flux at the Rosseland photosphere ($\tau_R = \frac{2}{3}$) of pure-H envelope models (*solid curve*) and pure-H atmosphere models (*dotted curves*) with log g = 7.5 and T_{eff} = 40,000 K (*top*), 70,000 K (*middle*), and 100,000 K (*bottom*).

element of interest with respect to H as given by Anders & Grevesse (1989) and Grevesse & Noels (1993). With one particularly outstanding exception, the predicted abundances from the two different approaches generally agree well, within 0.3 dex (although also some large differences exist at low values of T_{eff}, where the radiative support weakens considerably, thus producing a rapidly varying portion in the equilibrium abundance curves). The outstanding exception occurs when the physical conditions are such that a closed-shell electronic configuration dominates the ionization balance. This outcome is particularly evident for Mg, whose ionization state is dominated by Mg III for T_{eff} below ~60,000 K; Al, whose ionization state is dominated by Al IV in the range 30,000 K $\lesssim T_{eff} \lesssim$ 90,000 K; and Si, whose ionization state is dominated by Si V for T_{eff} above ~45,000 K (see Fig. 19 of CFW). When this situation happens, the true equilibrium abundances can be significantly *larger* than the abundances estimated by CFW, which can be readily understood. On the one hand, as discussed at length by CFW, the line opacity of a dominant noble gas ion occurs in the X-ray region. On the other hand, as shown in Figure 1, it is precisely in this region that the differences between the approximate and the exact Eddington flux are the largest. In this spectral range, the true flux is much larger than the approximate flux, and since no compensating effect exists at larger wavelengths for a noble gas ion because of the lack of opacity there, the equilibrium abundances must be larger under these conditions, as shown by the dashed curves. Note that, save for the hottest models, the X ray flux is generally quite small compared to the maximum in the energy distribution. This condition implies that the large differences obtained between the two approaches under noble gas conditions occur for abundances that are *small* in an absolute sense and that may be difficult to detect in practice.

2.2. *The Opacity of the Metal-enriched Atmospheric Plasma*

The representative chemical composition of the background plasma we consider consists of an H-dominated mixture with small traces (by number) of carbon (C/H = 4×10^{-7}), nitrogen (N/H = 5×10^{-6}), oxygen (O/H = 10^{-6}), and iron (Fe/H = 10^{-5}). The C and N abundances have been determined by Wesemael, Henry, & Shipman (1984), the O abundance by Chayer & Vennes (1995), and the Fe abundance by Vennes et al. (1992) and Werner & Dreizler (1994). These abundances are representative of the DA Feige 24.

The monochromatic opacity of the mixture has been computed by one of us (A. K. P.) for a range of physical conditions appropriate for computing a small set of model atmospheres of hot DA white dwarfs. These computations feature, in particular, the atomic physics and the equation of state employed in the Opacity Project, described by Seaton et al. (1994). The data consist of tables of the mixture's monochromatic opacity calculated at a fine mesh of 102,400 reduced-frequency ($u = h\nu/kT$) points for 88 pairs log N_e–log T in the electron density–temperature plane. Limits on the frequency grid are $u_{min} \simeq 3.162 \times 10^{-3}$ and $u_{max} \simeq 31.62$. We sample the calculated opacities to a linear accuracy of 1% for convenience in applica-

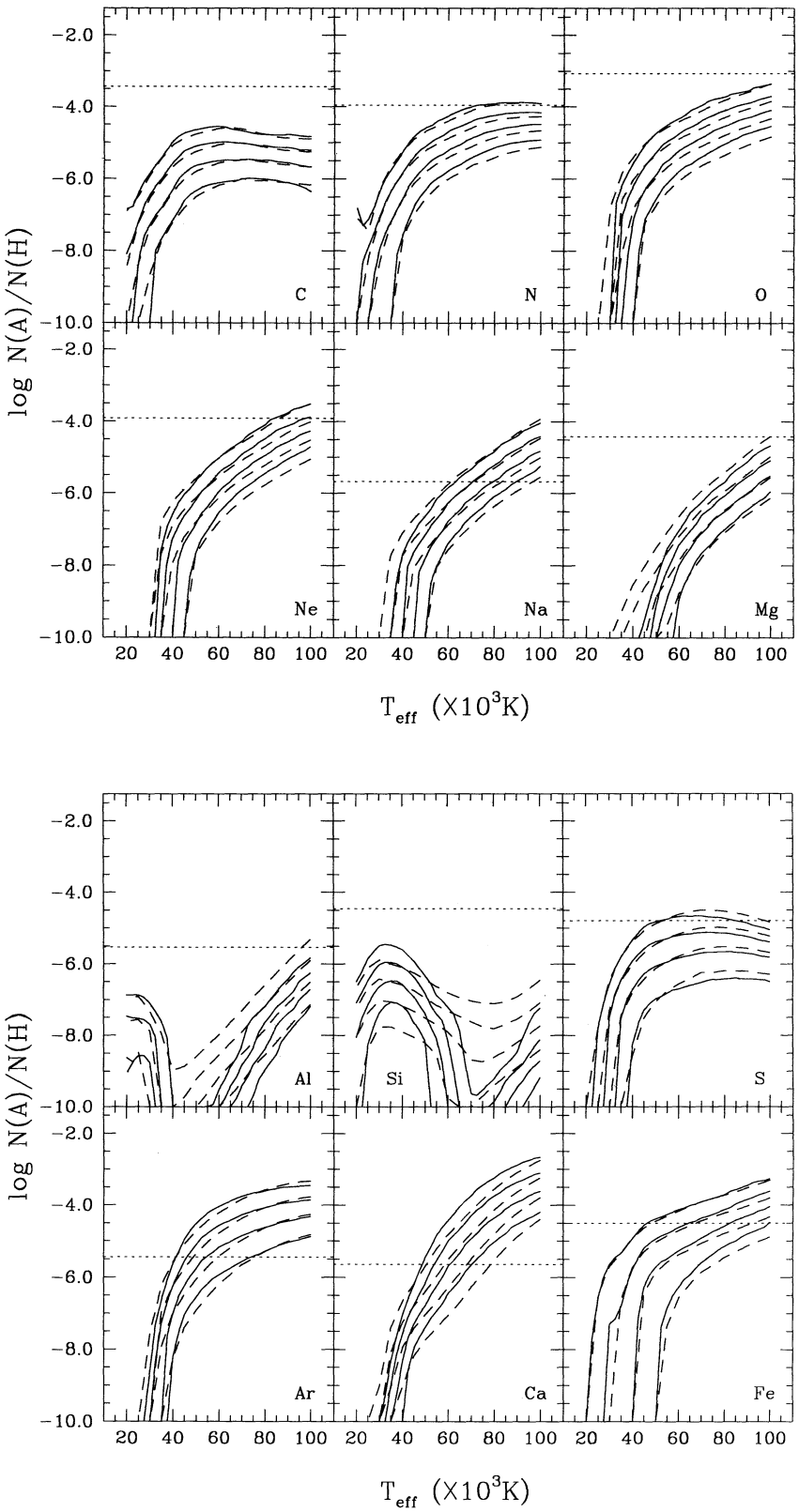

FIG. 2.—Expected equilibrium abundances of heavy elements levitating at the surface of hot DA white dwarfs. The equilibrium abundances are given with respect to that of H, by number. The figure shows the effects of the improvements brought about by considering a model-atmosphere approach (*dashed curves*) as compared to the results of a model-envelope approach (*solid curves*) for a pure-H background. From top to bottom, each series of curves refers to models with log g = 7.0, 7.5, 8.0, and 8.5. The horizontal dotted line in each panel gives the cosmic abundance of the element of interest.

tions and archiving. This procedure results in approximately 22,000 points, a factor of 5 less than the originally computed data, without any significant loss of accuracy in the retention of the highly resolved spectral features in the calculations.

Figure 3 illustrates some sample results for the monochromatic opacity. The panels refer to the physical conditions encountered at the Rosseland photosphere of a pure-H DA envelope model with log $g = 7.5$ and $T_{\rm eff} = 40{,}000$ K (*top*), 70,000 K (*middle*), and 100,000 K (*bottom*). These physical conditions are, respectively, log $N_e = 16.74$, 17.14, 17.48 and log $T = 4.60$, 4.85, 5.00. In each panel, the solid curve gives the detailed opacity of the mixture in the 0–200 Å wavelength range. In comparison, the dotted curve shows the minimal opacity produced by a pure-H plasma (as used by CFW) under the same conditions. Note that the dotted curve generally reproduces the lower envelope of the opacity of the mixture quite well, except at the shorter wavelengths, where Fe absorption dominates. Note also that little structure exists in the opacity of the mixture other than that caused by H for wavelengths larger than ~2000 Å (not shown); both curves essentially coincide for these wavelength regions, as the opacity of H completely dominates.

Figure 4 shows the behavior of the Rosseland mean opacity as a function of log g and $T_{\rm eff}$ for the conditions encountered at the photosphere of selected envelope models. The solid curves refer to models with log $g = 7.5$, the dashed curves to models with log $g = 8.0$. For each pair of curves, the upper one corresponds to the Rosseland opacity that we have computed for our mixture, while the lower one corresponds to the Rosseland opacity of a pure-H plasma. The latter data are taken directly from the envelope models constructed with the pure-H OPAL Rosseland opacity tables provided by Rogers & Iglesias (1992). Superposed on the lower curves are circles that give, for a few models, the Rosseland opacity computed from the pure-H monochromatic opacity used by CFW to calculate the background flux. These values show the excellent consistency between the two sets of data for pure H. As expected, because of the extra absorption by the trace elements (particularly Fe)

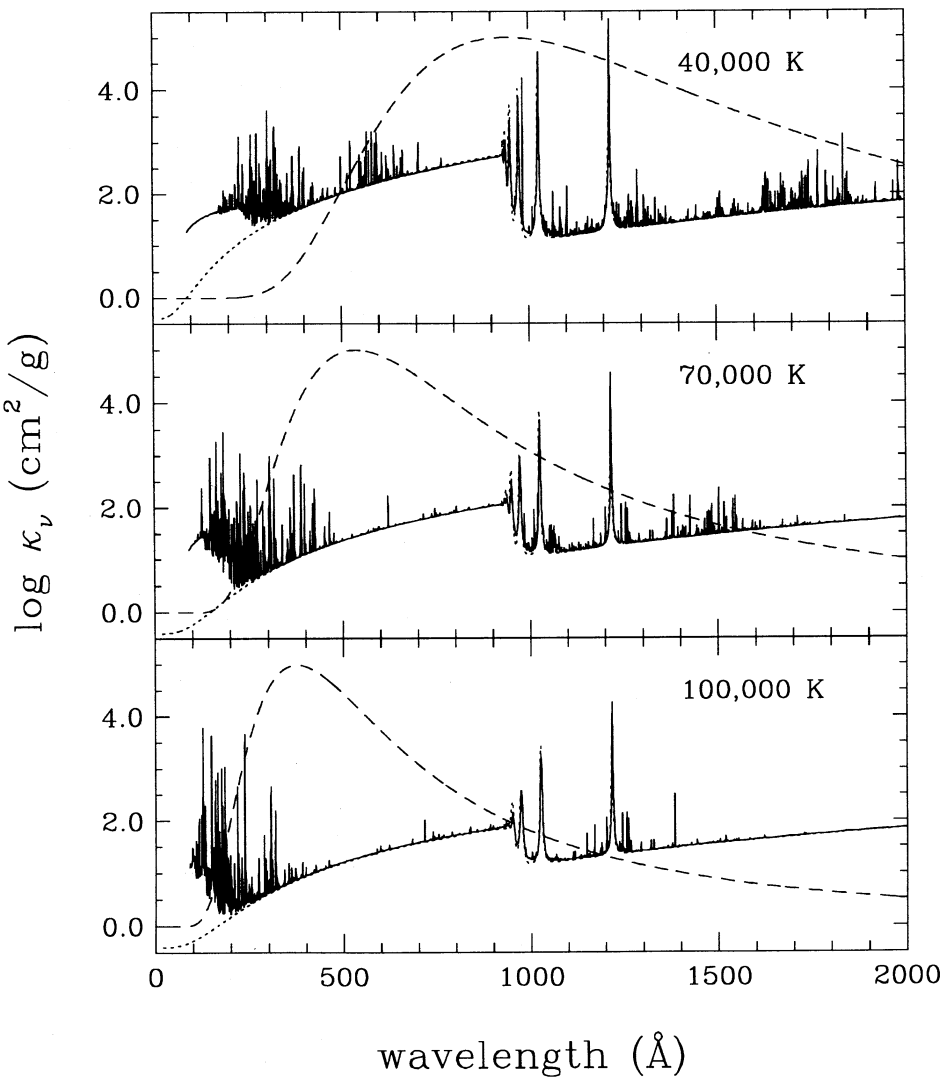

FIG. 3.—Comparison of the monochromatic opacity of the mixture (*solid curve*) with that of a pure-H plasma (*dotted curve*) calculated under the same physical conditions. The spectral window shown corresponds to wavelengths shorter than 2000 Å. The upper panels refer to the conditions encountered at the Rosseland photosphere of a pure-H envelope model with log $g = 7.5$ and $T_{\rm eff} = 40{,}000$ K (*top*), 70,000 K (*middle*), and 100,000 K (*bottom*). The dashed curve in each panel shows the Rosseland weighting function, normalized to a maximum value of 5.

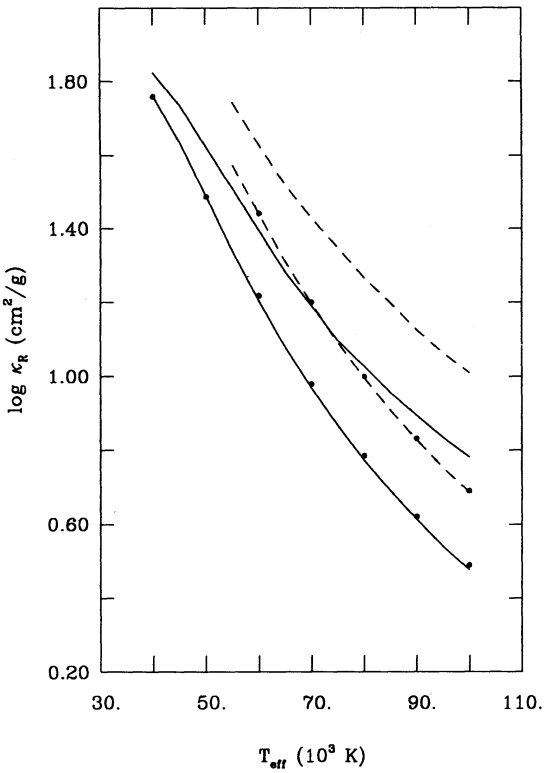

FIG. 4.—Comparison of Rosseland mean opacities calculated at the photosphere ($\tau_R = \frac{2}{3}$) of typical pure-H envelope models. The pair of solid curves refers to envelope models with log $g = 7.5$, the dashed curves to models with log $g = 8.0$. For each pair of curves, the upper one gives the Rosseland opacity of our mixture of H, C, N, O, and Fe, and the lower curve gives instead the Rosseland opacity of a pure-H plasma calculated under the same conditions, taken from the OPAL data; the superposed circles correspond to the Rosseland opacity derived from the monochromatic opacity of a pure-H plasma, calculated as in CFW.

in the mixture, the Rosseland opacity is larger for that mixture than for pure H. To understand why the differences are larger at higher effective temperatures, the reader may refer back to Figure 3, where we have plotted (*dashed curve*), in each panel, the Rosseland weighting function

$$w(u) = \frac{15}{4\pi^4} \frac{u^4 e^u}{(e^u - 1)^2}, \quad (3)$$

arbitrarily normalized to a maximum value of 5. It is clear that, as T_{eff} increases, the weighting function shifts to shorter wavelengths and, therefore, increasingly samples the soft X-ray regions, where Fe absorption dominates in the mixture. Hence, The Rosseland opacity becomes more sensitive to the presence of trace contaminants with increasing effective temperature.

2.3. *Hydrogen-rich Models with Trace Heavy Elements*

The opacity tables were originally constructed to compute a small grid of model atmospheres suitable for the analysis of the hot DA star Feige 24 and its siblings (G191-B2B, RE 2214-492, and RE 0623-377), all of which have comparable atmospheric parameters. The models have log $g = 7.5$ or 8.0 and $T_{eff} =$ 52,000, 56,000, 60,000, or 64,000 K. They are LTE models and include a detailed treatment of blanketing effects through the use of some 30,000 frequency points. This choice was made in order to oversample the monochromatic opacity given in the tables. The models were computed by Vennes, Pradhan, & Thejll (1995), and details are provided there. They will be referred to as the *HZ models* in what follows.

We now take advantage of the availability of the HZ models to consider the question of flux redistribution in the presence of trace pollutants in a radiative levitation context. Specifically, we use the available stratifications to compute the Eddington flux at the Rosseland photosphere of the HZ models and then incorporate this flux in radiative acceleration calculations to eventually obtain representative atmospheric equilibrium abundances of the 12 heavy elements of interest in this study. In order to provide a comparison point, we also make use of pure-H model atmospheres similar to those described in § 2.1, but computed on the same small grid as the HZ models; they will be referred to as the *H models* in the following.

Figure 5 illustrates the differences in the Eddington flux at $\tau_R = \frac{2}{3}$ between HZ models (*solid curves*) and H models (*dotted curves*) with log $g = 7.5$ and $T_{eff} = 52{,}000$ K (*top*) and 64,000 K (*bottom*). The extra opacity of the trace elements in the mixture causes a redistribution of the flux in the HZ models such that the *continuum* flux of these models is *larger* than that of the corresponding H models for $\lambda \gtrsim 200$ Å. At shorter wavelengths, however, the flux of the HZ models plummets to very low values compared to that of the H models. Of course, the flux in the lines of C, N, O, and Fe (the trace constituents in the mixture used to compute the HZ models) can be smaller than that available in the energy distribution of pure-H models at the appropriate wavelengths.

We compare, in Figure 6, the predicted atmospheric abundances of our 12 standard heavy elements as functions of the surface gravity and the effective temperature of the HZ (*dashed curves*) and H (*solid curves*) atmosphere models. The expected equilibrium abundances of S, Ar, and Ca are larger, while those of Na, Mg, Al, and Fe are smaller in the presence of a contaminated background plasma as compared to the pure-H case. Likewise, the abundances of Ne are comparable for the two kinds of background. For the levitating elements that do not belong to the background mixture (i.e., those other than C, N, O, and Fe), and except for possible accidental occurrences, the narrow absorption lines generally fall in the continuum of the energy distribution of an HZ model. For the needs of the present discussion, this "continuum" also includes the relatively broad H lines present in both the HZ and H models. Because the continuum flux of an HZ model is larger than that of a comparable H model for $\lambda \gtrsim 200$ Å, and the converse is true for shorter wavelengths, a heavy element will receive more (less) radiative support in an HZ model if its line opacity is more (less) important in the spectral region $\lambda \gtrsim 200$ Å than in the spectral region $\lambda \lesssim 200$ Å.

Examples of this behavior are shown in Figure 7, where, in the top panel, we have plotted the line opacity of Mg IV, the dominant ion of Mg, at the Rosseland photosphere of an HZ model atmosphere with log $g = 7.5$ and $T_{eff} = 60{,}000$ K. We assumed a solar abundance Mg/H $= 3.8 \times 10^{-5}$ here and included 2263 bound-bound transitions. This result is to be compared to the curves in the bottom panel, which show, in a format similar to Figure 5, the Eddington flux at $\tau_R = \frac{2}{3}$ of the HZ model (*solid curve*) and that of the corresponding H model (*dotted curve*). While Mg IV shows some opacity over a wide spectral range, its strongest bound-bound transitions occur at relatively short wavelengths, where the flux of the HZ model is less than that of the H model. As a result, the radiative support on, and the equilibrium abundance of, Mg is smaller for the HZ model. In contrast, the middle panel, which illustrates the

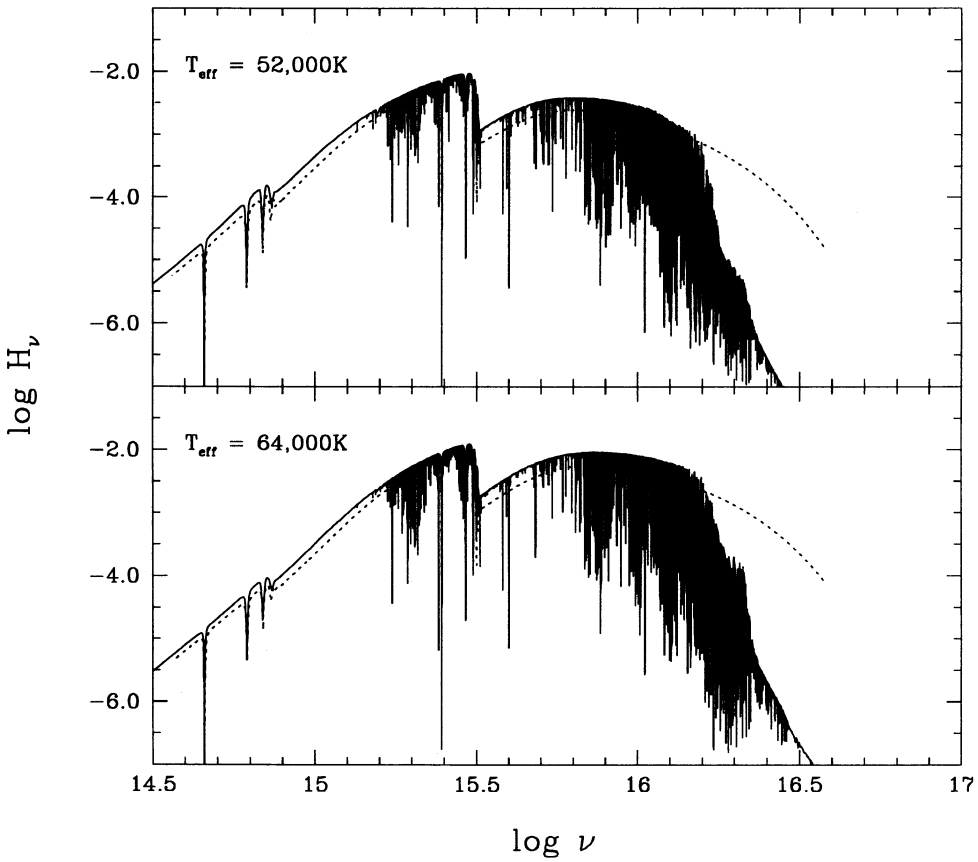

FIG. 5.—Eddington flux at the Rosseland photosphere ($\tau_R = \frac{2}{3}$) of H (*dotted curves*) and HZ (*solid curves*) model atmospheres with log $g = 7.5$ and $T_{eff} = 52{,}000$ K (*top*) and 64,000 K (*bottom*).

distribution of the line opacity of Ar V (responsible for most of the radiative support on Ar in this particular model atmosphere), indicates that this ion is preferentially opaque at $\lambda \gtrsim 200$ Å, so its equilibrium abundance is larger for the HZ model. Again, the solar abundance (Ar/H = 3.6×10^{-6}) was used in the opacity calculation, and 6357 transitions were considered.

Let us consider next the remaining cases of the levitating elements that also belong to the background mixture (C, N, O, and Fe). For the range of atmospheric parameters covered, Figure 6 reveals that the abundances of C, N, and O are essentially the same in the HZ models as in the corresponding H models. Also, as expected, Fe, as the dominant source of the extra opacity, is less supported in the HZ models. To understand these results, it is important to realize that the flux in the lines of C, N, and O in our particular examples is not necessarily always smaller than the flux provided by a pure-H plasma. This flux depends on the details of the redistribution process (which is largely specified here by the opacity of Fe) and the assumed abundances of the elements in the mixture. By coincidence, the equilibrium abundances of C, N, and O turn out to be quite similar in the Hz and the H models considered in this paper.

In ending this section, we emphasize once more that the results obtained here can only be considered as *illustrative*. Some inconsistencies exist, for instance, between the assumed abundances of C, N, O, and Fe in the background mixture and the derived equilibrium abundances of the same elements. Likewise, the other levitating elements that we have considered must, if present, affect the background flux as well. As indicated in § 1, however, and until the exact atmospheric chemical composition of a white dwarf is determined, a self-consistent computation cannot be carried out. This situation also implies that individual stars will have to be analyzed case by case.

3. OTHER IMPROVEMENTS

In an important paper, Gonzalez et al. (1995) recently discussed a number of improvements in the computation of radiative accelerations in stellar envelopes. While these new results came too late to be incorporated into the bulk of the calculations presented by CFW, the latter authors were nevertheless able to assess the impact of these developments on their results. It turns out that, along with the questions considered in § 2 above, the last significant problem in the context of equilibrium radiative levitation theory in white dwarfs is how to describe the momentum redistribution process following the absorption of a photon by an ion. In the method used by CFW, the probabilities that the newly gained momentum of the excited ion is spent either in its initial ionization state i or in the higher state $i + 1$ are assigned to the ion as *a whole*. In contrast, in the improved discussion of Gonzalez et al. (1995), such probabilities are assigned to *each and every* individual radiative transition considered in the calculation of the radiative acceleration. Moreover, Gonzalez et al. (1995) show that all previous studies (including the work of CFW) have underestimated the effects of electronic collisions on the ionization

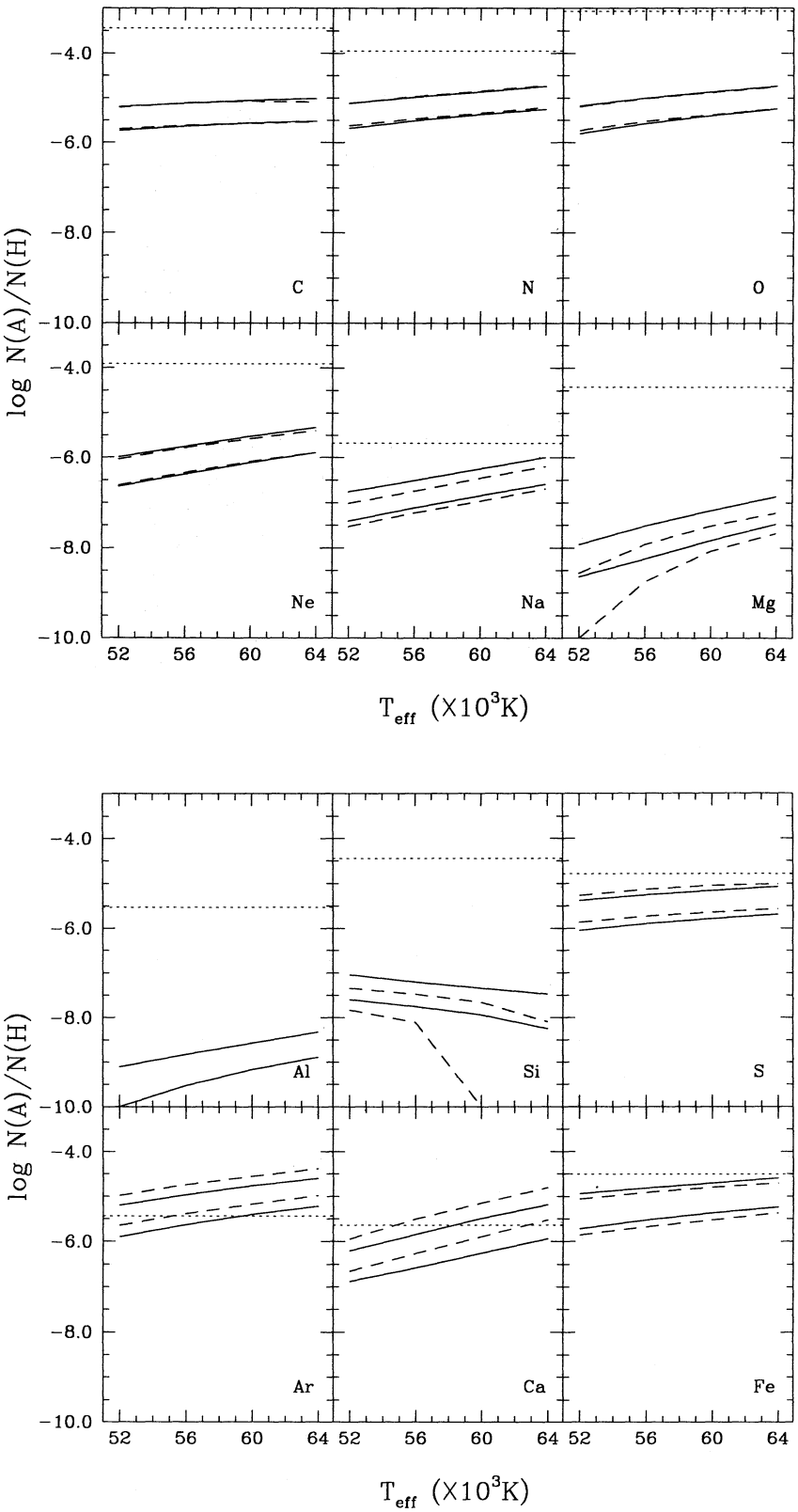

FIG. 6.—Expected equilibrium abundances of heavy elements levitating at the surface of hot DA white dwarfs. The figure illustrates the effects of using the contaminated background (*dashed curves*) as compared to the case of a pure-H background (*solid curves*). The upper pair of curves refers to model atmospheres with log $g = 7.5$, the lower pair to models with log $g = 8.0$.

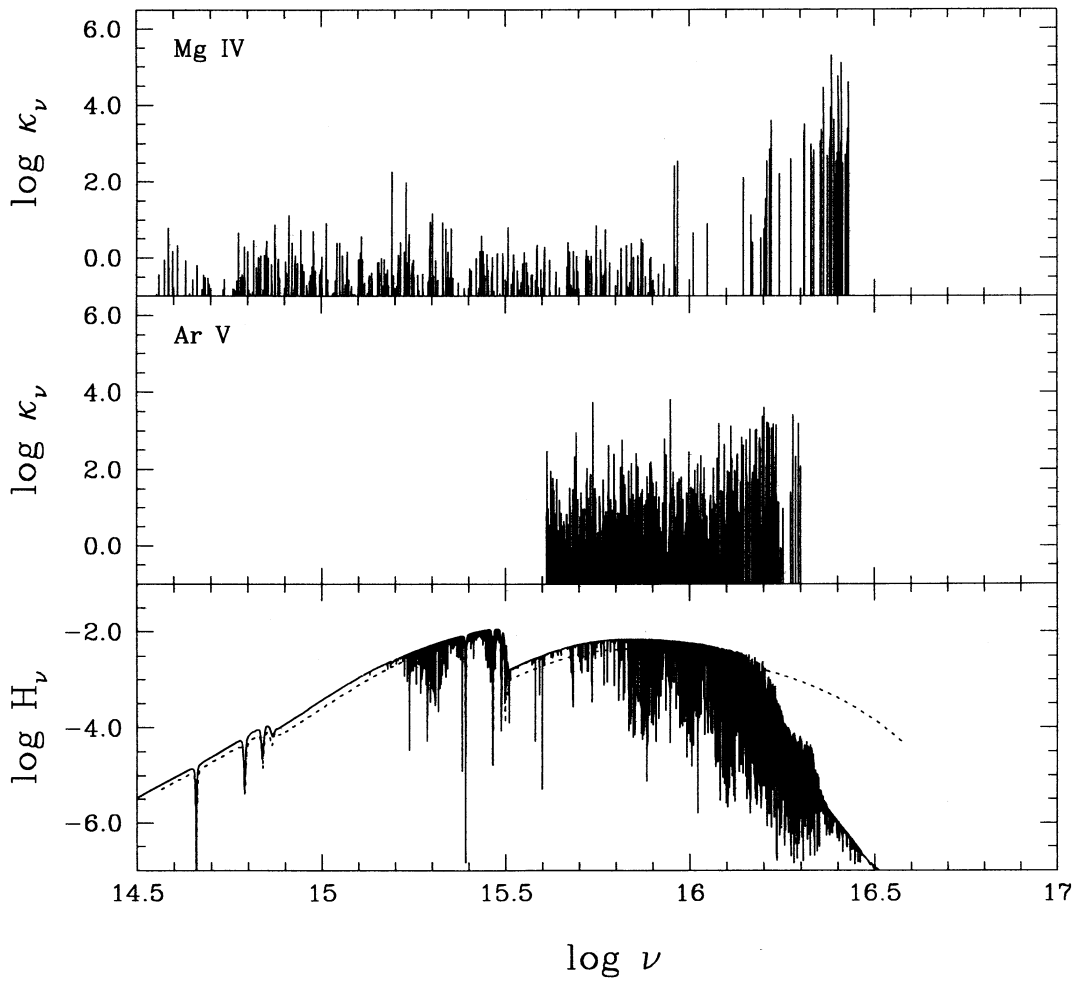

FIG. 7.—Line opacity and Eddington flux at the Rosseland photosphere of model atmospheres with log $g = 7.5$ and $T_{\rm eff} = 60{,}000$ K. The top and middle panels show, respectively, the line opacities of Mg IV and Ar V at the photosphere of the HZ model; these two ions are responsible for most of the radiative support on these elements. Cosmic abundances have been assumed to evaluate these opacities. In comparison, the Eddington flux of both the HZ (*solid curve*) and H (*dotted curve*) atmosphere models is shown in bottom panel.

rates. As a result, the improved treatment of Gonzalez et al. (1995) leads to a momentum redistribution process that tends to favor the higher ionization state $i + 1$. In contrast, most of the newly gained momentum is spent in state i in the method used by CFW. Because the higher ionization state $i + 1$ is less mobile than state i (its higher charge leads to a larger interaction with the background plasma), the prescription of Gonzalez et al. (1995) leads to *smaller* radiative accelerations than does the method used by CFW and many others before. CFW estimated that the incorporation of the new and detailed treatment proposed by Gonzalez et al. (1995) would lead to a systematic reduction of the equilibrium abundances by, typically, a factor of ~ 3, with some variations from one element to another (which can only be obtained through actual calculations).

To follow up on the work of CFW, we present the results of additional calculations that incorporate the detailed recipe proposed by Gonzalez et al. (1995). Thus, for the bound-bound transitions of an ion of type i ending in a state for which the principal quantum number of the active electron is equal to that of the ground state plus one, the ionization probability is zero (the momentum gained in such transitions is spent in ionization state i). For all the other transitions, the ionization probability is set to one (the momentum is spent in ionization state $i + 1$). Along with this improved prescription, our calculations also incorporate a more minor change also suggested by the work of Gonzalez et al. (1995). Specifically, what we have done so far (and in CFW), the full width at half-maximum of the Lorentz profile resulting from pressure broadening—which is a component of the Voigt profile used to describe the absorption lines—has been the semiempirical expression of Alecian, Michaud, & Tully (1993). According to the work of Gonzalez et al. (1995), though, a change of the numerical constant appearing in the front of this expression (see eq. [7] of CFW) from 6.3×10^{-6} to 8.0×10^{-6} gives a somewhat better fit to the results of the sophisticated broadening theory developed by Dimitrijević & Konjević (1980, 1986, 1987). This change leads to a relatively small but systematic *increase* of the radiative accelerations and equilibrium abundances.

In a now familiar format, Figure 8 compares the predicted surface equilibrium abundances of our 12 selected heavy elements calculated according to our past standard procedure (*solid curves*) to those calculated according to the improved just described (*dashed curves*). In both cases, the Eddington flux used in the radiative acceleration calculations was taken from our grid of pure-H model atmospheres, briefly described in § 2.1. We observed that the improved estimates of the equilibrium abundances are generally systematically smaller than

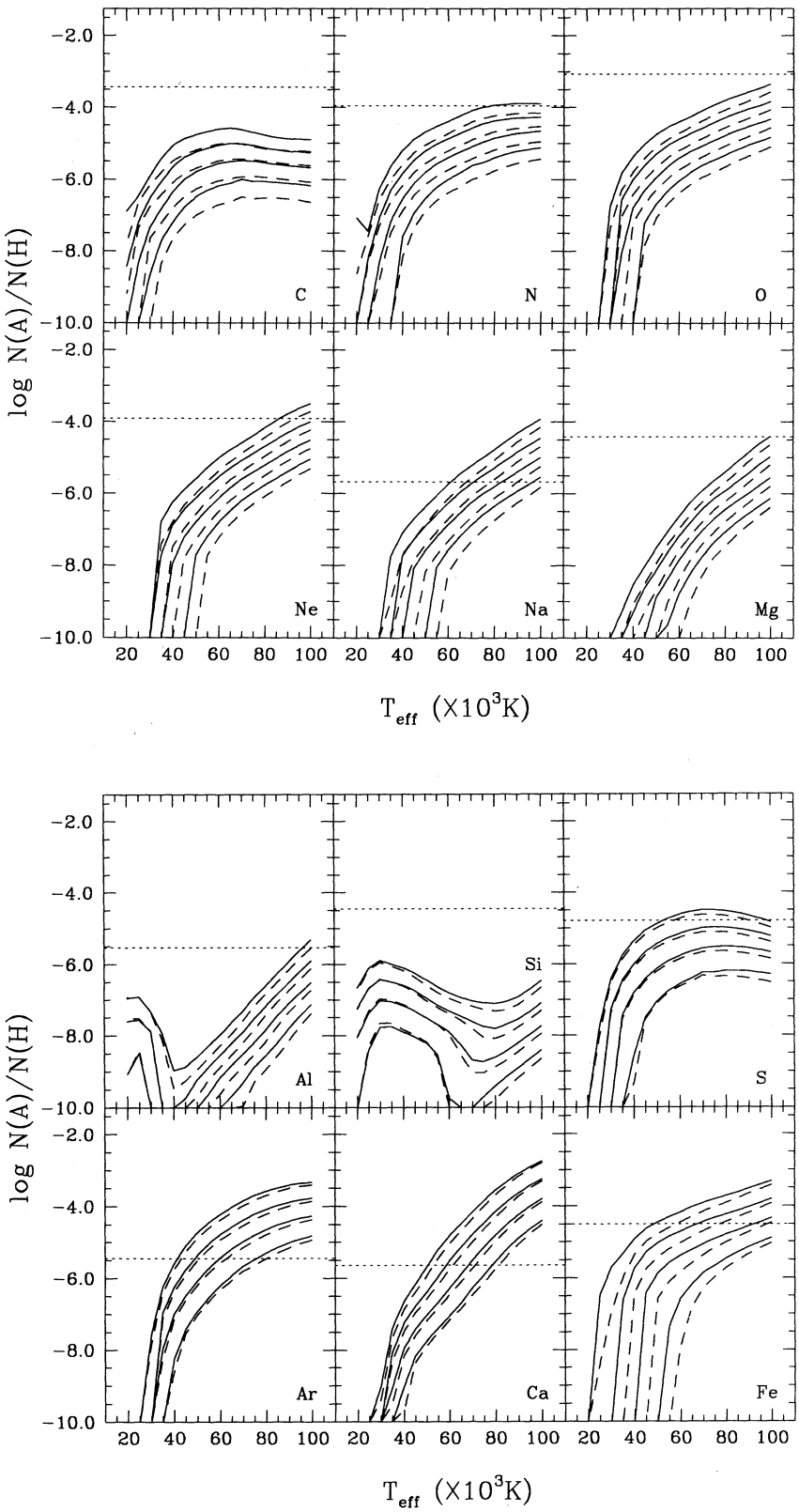

FIG. 8.—Expected equilibrium abundances of heavy elements levitating at the surface of hot DA white dwarfs. The figure illustrates the effects of the improvements brought about by considering the upgrades of Gonzalez et al. (1995) (*dashed curves*) as compared to our standard procedure (*solid curves*). Both sets of curves refer to the pure-H background in the model-atmosphere approach. The format is otherwise similar to that of Fig. 2.

before, indicating that the momentum redistribution process of Gonzalez et al. (1995) is the dominant new mechanism. (A few exceptions arise for Si at low values of $T_{\rm eff}$.) Taking into account the contributing effects of increasing the line width (which leads to an increase in the equilibrium abundances), we find that the estimate of CFW, which suggests an overall decrease of the abundances by a factor of ~ 3 due to the momentum redistribution process, is quite realistic.

Very similar results are obtained when considering our mixtures of H with small traces of C, N, O, and Fe, as shown in Figure 9, where the equilibrium abundances have been computed on the basis of the synthetic fluxes derived from our small grid of HZ model atmospheres. As in Figure 8, the dashed curves give the abundances obtained from our improved procedure for computing radiative forces, and the solid curves refer to the somewhat less sophisticated procedure used in the previous sections.

In a final numerical experiment, we have investigated the effects of adding some He to our mixture of pollutants (C, N, O, and Fe). While He has not been detected in the four hot DA white dwarfs with a reported presence of heavy elements (Feige 24, G191-B2B, RE 2214-492, and RE 0623-377), it is present in the metal-rich DAO star Feige 55 at the level He/H $\simeq 10^{-3}$ (Bergeron et al. 1994), which is significantly larger than the abundances we have used for C, N, O, and Fe. Using this abundance, we have computed another detailed blanketed model atmosphere, with a composition made of H, He, and our standard mixture of heavy elements. This model has $\log g = 7.5$ and $T_{\rm eff} = 60{,}000$ K. On the basis of the Eddington flux calculated in this model, we have next obtained, as usual, the equilibrium abundances of our 12 standard elements using our improved procedure for computing the radiative accelerations. Comparing the corresponding results in Figure 9, we find that the addition of He (even in much larger proportions than C, N, O, and Fe) has only minor effects, thus confirming the central role of the much more opaque Fe atom. For the record, the abundances of all the elements, except Ar and Ca, are smaller when He is added to the background plasma. On average, the change in the equilibrium abundance is only 15.5%, with an rms deviation of $\pm 12.4\%$.

It is of interest, at this point, to verify whether our improved calculations lead to predicted equilibrium abundances that better agree with the observations. Verification can best be done in the case of Feige 24, since the abundances of C, N, O, and Fe assumed for the mixture of contaminants used here are those inferred in previous abundance analyses carried out for that star. Unfortunately, out of the 12 heavy elements considered in this paper, only Si can be added to the short list of elements for which abundances have been determined in Feige 24. Thus, in Figure 10, we compare the abundances of C, N, O, Si, and Fe derived from various published abundance analyses and averaged as in CFW (*filled circles*) to the predicted abundances according to CFW (*open circles joined by a dashed line*). The CFW data are from CFW's Figure 21 (*lower panel*), with the Fe abundance taken from the TOPBASE calculations. Our best estimates are obtained from the appropriate data in Figure 9 and incorporate all the improvements discussed in this paper (namely, atmospheric models with trace heavy elements and improved treatment of the momentum redistribution process). In both cases, the predicted abundances have been obtained by interextrapolation on model grids using $\log g = 7.29$ and $T_{\rm eff} = 54{,}300$ K as best estimates for the atmospheric parameters of Feige 24 (see Table 6 of CFW). Note, furthermore, that all equilibrium abundances discussed in this paper are based on the TOPBASE data set and, as such, are computed without taking into account the fine structure in the atomic transitions. Such more involved calculations are currently only possible (from a practical point of view) for the Fe-group elements, whose atomic data have been compiled by Kurucz (1991, 1992). Chayer et al. (1994) have used these data to compute equilibrium abundances of Fe and Ni in the atmospheres of hot DA stars. Since the fine structure acts as a broadening mechanism and somewhat desaturates a multiplet transition, *higher* equilibrium abundances are derived. Unfortunately, except for Fe and Ni, we do not know by how much the abundances of our other elements of interest may increase.

We find it interesting that the results of Figure 10 indeed suggest that our improved calculations agree with the observations better than previous results (at least in the case of Feige 24). For instance, our predicted abundances of N and Fe now essentially fall on the observed values. The expected abundances of C and O are still larger than the observed values, but the disagreement has been substantially reduced. In contrast, the predicted abundance of Si is practically unchanged compared to the earlier estimate of CFW and is still somewhat too small to be consistent with the observations. While the overall results are quite encouraging, they should be interpreted in the broader context of the spectral evolution of white dwarfs. For instance, as discussed at some length in CFW, we know that the predictions of *equilibrium* radiative levitation theory cannot account for the *bulk* of the observations in hot white dwarfs. The improvements discussed in this paper do not change this basic conclusion. Other mechanisms (possibly with variable efficiency from star to star) are at work in hot white dwarfs. Hence, while equilibrium radiative levitation theory appears to give reasonable results for Feige 24 (although the results for C, O, and Si are admittedly not perfect), it does not account for what is observed in many other white dwarfs, including objects with atmospheric parameters similar to those of Feige 24.

4. CONCLUSION

In their concluding remarks, CFW suggest a number of avenues for improving the calculation of radiative accelerations in the context of equilibrium radiative levitation theory in hot white dwarfs. We have addressed these issues here, and the present effort can be considered to complement the work of CFW. By neglecting, in a first approximation, the effects of trace heavy elements on the background flux, we find improved estimates for the equilibrium abundances of our 12 standard heavy elements expected at the surface of hot DA white dwarfs, illustrated by the dashed curves in Figure 8. The improvements involved are related to our use of (1) model atmospheres to compute the exact Eddington flux at the Rosseland photosphere, (2) the more sophisticated treatment of the momentum redistribution process that an ion experiences following a photoexcitation described by Gonzalez et al. (1995), and (3) a slightly revised width for the line profile associated with pressure broadening, also as discussed by Gonzalez et al. (1995). These improvements, coupled with our use of the TOPBASE atomic data, and under the assumption of a pure-H background plasma, upgrade our estimates of equilibrium abundances to the state-of-the-art level in the field. We note, in this context, several improvements underway in the atomic data calculation and the computation of opacities, including new, improved radiative calculations for the photoionization cross sections and transition probabilities for the important low-ionization states of iron, Fe I–Fe V, under the

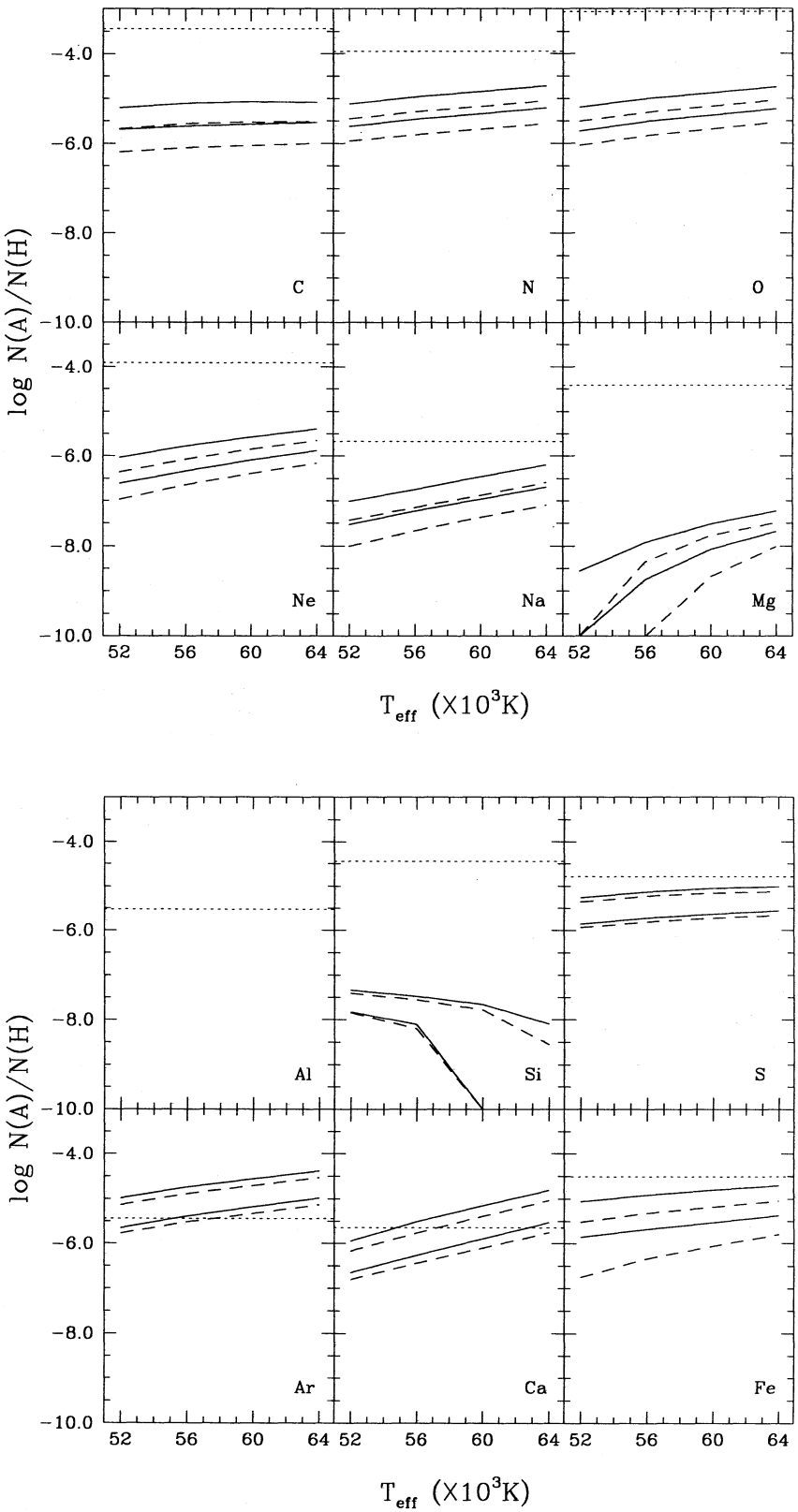

FIG. 9.—Similar to Fig. 8, but for the smaller grid of model atmospheres computed for the contaminated background plasma. The format is similar to that of Fig. 6.

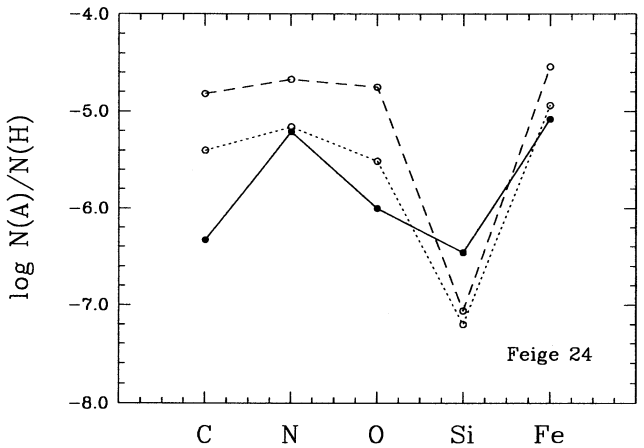

FIG. 10.—Comparison of the observed (*filled circles*) and expected (*open circles*) abundances of C, N, O, Si, and Fe in Feige 24. The dotted line refers to the improved calculations discussed in this paper, while the dashed line refers to the earlier results of CFW.

Iron Project (Hummer et al. 1993) and the incorporation of fine-structure splitting in the Russell-Saunders (LS) coupling multiplet transition probabilities (not available in the current TOPBASE data set).

In a more realistic approach, the effects of trace pollutants on the background flux must be taken into account. This is a complex problem, since it involves an a priori knowledge of the atmospheric chemical composition of a hot white dwarf, which, unfortunately, is currently only partially available for a few objects. Short of a fully-fledged, self-consistent computation, we have taken advantage of a small grid of monochromatic opacities appropriate for an H-rich plasma contaminated by small traces of C, N, O, and Fe to explore how the equilibrium abundances of levitating elements react to the flux redistribution brought about by the extra opacity of trace elements in the background mixture. Our "best" results, incorporating the three improvements mentioned in the previous paragraph, are given by the dashed curves in Figure 9. We again emphasize that these results can only be considered as *illustrative* because of the inconsistencies between the fixed chemical composition of the background plasma and the derived equilibrium abundances of the various heavy elements. They show, however, that the relative abundances of levitating elements can be significantly altered, particularly in the present examples, by the presence of an opaque element such as Fe. This reaction suggests that other elements of the Fe group may also have some important influence in the theory of radiative support.

Our use of model atmospheres, which was essential to describe the flux redistribution process exactly, has allowed us to compare directly the predicted atmospheric abundances of levitating elements obtained on the basis of a model-envelope approach (as in CFW) to those obtained on the basis of a model-atmosphere approach. Comparison was carried out for a pure-H background plasma (see Fig. 2). Except for the cases in which the dominant ionization state at the photosphere corresponds to a closed-shell configuration, we found that the model-envelope approach gives quite reasonable estimates of *atmospheric* abundances of levitating elements. This result is of some importance because the model-envelope approach is the method of choice in more complicated descriptions of hot white dwarfs, such as those calling upon time-dependent calculations involving radiative levitation in the presence of stellar winds or accretion.

Finally, we point out that the improvements described in this paper have found their application in the relatively simple context of *equilibrium* radiative levitation theory. Our revised estimates of the surface abundances of levitating elements in hot DA stars do not change the fundamental conclusion reached by CFW: equilibrium radiative levitation theory, however, sophisticated, cannot account for the bulk of the available observations, and, consequently, other mechanisms must be simultaneously at work in these stars.

We are particularly indebted to P. Bergeron for enlightening discussions. We also acknowledge financial support from the Natural Sciences and Engineering Research Council of Canada and from the fund FCAR (Québec). A. K. P. acknowledges partial support from the US National Science Foundation (PHY-9115057). P. T. acknowledges support from the Carlsberg Foundation. This work was supported by NASA contract NAS 5-30180.

REFERENCES

Alecian, G., Michaud, G., & Tully, J. 1993, ApJ, 411, 882
Anders, E., & Grevesse, N. 1989, Geochim. Cosmochim. Acta, 53, 197
Bergeron, P., Wesemael, F., Beauchamp, A., Wood, M. A., Lamontagne, R., Fontaine, G., & Liebert, J. 1994, ApJ, 432, 305
Bergeron, P., Wesemael, F., Michaud, G., & Fontaine, G. 1988, ApJ, 332, 964
Chayer, P., Bergeron, P., Fontaine, G., & Wesemael, F. 1989a, JRASC, 83, 325
Chayer, P., Fontaine, G., & Wesemael, F. 1989b, in IAU Colloq. 114, White Dwarfs, ed. G. Wegner (New York: Springer), 253
———. 1995, ApJS, 99, 189
Chayer, P., LeBlanc, F., Fontaine, G., Wesemael, F., Michaud, G., & Vennes, S. 1994, ApJ, 436, L161
Chayer, P., & Vennes, S. 1995, in preparation
Cunto, W., & Mendoza, C. 1992, Rev. Mexicana Astron. Astrofiz., 23, 107
Dimitrijević, M. S., & Konjević, N. 1980, J. Quant. Spectrosc. Rad. Transfer, 24, 451
———. 1986, A&A, 163, 297
———. 1987, A&A, 172, 345
Gonzalez, J.-F., LeBlanc, F., Artru, M.-C., & Michaud, G. 1995, A&A, 297, 223
Grevesse, N., & Noels, A. 1993, in Origin and Evolution of the Elements, ed. N. Prantzos, E. Vangioni-Flam, & M. Cassé (Cambridge: Cambridge Univ. Press), 15
Holberg, J. B., et al. 1993, ApJ, 416, 806
Holberg, J. B., Hubeny, I., Barstow, M. A., Lanz, T., Sion, E. M., & Tweedy, R. W. 1994, ApJ, 425, L105
Hummer, D. G., Berrington, K. A., Eissner, W., Pradhan, A. K., Saraph, H. E., & Tully, J. A. 1993, A&A, 279, 298
Hummer, D. G., & Mihalas, D. 1988, ApJ, 331, 794
Kurucz, R. L. 1991, in Stellar Atmospheres, ed. L. Crivellari, I. Hubeny, & D. G. Hummer (NATO ASI Ser. C, 341) (Dordrecht: Kluwer), 441
———. 1992, Rev. Mexicana Astron. Astrofiz., 23, 45
Napiwotzki, R., Barstow, M. A., Fleming, T., Holweger, H., Jordan, S., & Werner, K. 1993, A&A, 278, 478
Rogers, F. J., & Iglesias, C. A. 1992, ApJS, 79, 507
Seaton, M. J., Yu, Y., Mihalas, D., & Pradhan, A. K. 1994, MNRAS, 266. 805
Seaton, M. J., Zeipper, C. J., Tully, J. A., Pradhan, A. K., Mendoza, C., Hibbert, A., & Berrington, K. A. 1992, Rev. Mexicana Astron. Astrofiz., 23, 19
Sion, E. M., Liebert, J., & Wesemael, F. 1985, ApJ, 292, 477
Vennes, S. 1992, ApJ, 390, 590
Vennes, S., Chayer, P., Fontaine, G., & Wesemael, F. 1989, ApJ, 336, L25
Vennes, S., Chayer, P., Thorstensen, J. R., Bowyer, S., & Shipman, H. L. 1992, ApJ, 392, L27
Vennes, S., Pradhan, A. K., & Thejll, P. 1995, in preparation
Vennes, S., Thejll, P., & Shipman, H. L. 1991, in White Dwarfs, ed. G. Vauclair & E. M. Sion (Dordrecht: Kluwer), 235
Vidal-Madjar, A., Allard, N. F., Koester, D., Lemoine, M., Ferlet, R., Bertin, P., Lallement, R., & Vauclair, G. 1994, A&A, 287, 175
Werner, K., & Dreizler, S. 1994, A&A, 286, L31
Werner, K., Dreizler, S., & Wolf, N. 1995, A&A, 298, 567
Werner, K., Heber, U., & Fleming, J. 1994, A&A, 284, 907
Wesemael, F., Auer, L. H., Van Horn, H. M., & Savedoff, M. P. 1980, ApJS, 43, 159
Wesemael, F., Henry, R. B. C., & Shipman, H. L. 1984, ApJ, 287, 868